Journal of Quantitative Spectroscopy & Radiative Transfer ▮ (▮▮▮▮) ▮▮▮–▮▮▮

Contents lists available at SciVerse ScienceDirect

Journal of Quantitative Spectroscopy & Radiative Transfer

journal homepage: www.elsevier.com/locate/jqsrt

Atmospheric absorption of terahertz radiation and water vapor continuum effects

David M. Slocum [a,*], Elizabeth J. Slingerland [a,b], Robert H. Giles [a], Thomas M. Goyette [a]

[a] Submillimeter-Wave Technology Laboratory, University of Massachusetts Lowell, 175 Cabot St Ste 130 Lowell, MA 01854, United States
[b] Metron Inc., 1818 Library St Ste 600, Reston, VA 20190, United States

ARTICLE INFO

Article history:
Received 21 February 2013
Received in revised form
11 April 2013
Accepted 21 April 2013

Keywords:
Water vapor
Absorption
Continuum
Terahertz
Spectroscopy

ABSTRACT

The water vapor continuum absorption spectrum was investigated using Fourier Transform Spectroscopy. The transmission of broadband terahertz radiation from 0.300 to 1.500 THz was recorded for multiple path lengths and relative humidity levels. The absorption coefficient as a function of frequency was determined and compared with theoretical predictions and available water vapor absorption data. The prediction code is able to separately model the different parts of atmospheric absorption for a range of experimental conditions. A variety of conditions were accurately modeled using this code including both self and foreign gas broadening for low and high water vapor pressures for many different measurement techniques. The intensity and location of the observed absorption lines were also in good agreement with spectral databases. However, there was a discrepancy between the resonant line spectrum simulation and the observed absorption spectrum in the atmospheric transmission windows caused by the continuum absorption. A small discrepancy remained even after using the best available data from the literature to account for the continuum absorption. From the experimental and resonant line simulation spectra the air-broadening continuum parameter was calculated and compared with values available in the literature.

1. Introduction/Background

The Earth's atmosphere is full of absorbing species. Many of these species can render the atmosphere nearly opaque in specific frequency bands. Water for example has hundreds of rotational and vibrational absorption lines from the radio wave range through the terahertz region. Since water vapor pervades the entire atmosphere, the propagation of radiation can only occur in parts of the electromagnetic spectrum that is not wholly absorbed by water. These atmospheric windows are located between the strong resonant absorption lines; however, some radiation is still absorbed even in the atmospheric windows. Water vapor absorption is usually separated in two parts to describe this phenomenon, absorption due to the resonant rotational or vibrational lines and that due to the continuum. Continuum absorption is most often empirically determined and defined as the difference between the experimentally observed spectrum and the calculated resonant absorption line spectrum.

Much work has been performed to characterize and understand the absorption peaks of water vapor [1–3] as well as to determine the functional form of the continuum contribution to water vapor absorption in the terahertz regime [4–8]. The continuum contribution to the absorption coefficient scales as the square of the frequency and has a negative dependence on temperature in the microwave [8–10], however, at higher frequencies only a limited

* Corresponding author. Tel.: +1 978 934 1300.
E-mail address: david_slocum@student.uml.edu (D.M. Slocum).

0022-4073/$ - see front matter © 2013 Elsevier Ltd. All rights reserved.
http://dx.doi.org/10.1016/j.jqsrt.2013.04.022

number of studies have shown a quadratic dependence on frequency in the terahertz regime [11–13]. Further complicating the continuum absorption, there is uncertainty as to the values of the continuum parameters within any given model. This ambiguity is due to the heavy dependence of the parameters on the line shape function and the number of absorption lines used in the model as well as a limited number of experimental studies at terahertz frequencies. The water vapor absorption spectrum has been extensively studied, but until recently the terahertz region of the spectrum has received little attention for experimental work. Only a few broadband studies have been performed in the terahertz region, most of which were performed in a laboratory environment using either pure nitrogen or oxygen gas as the foreign broadening gas [12–15]. This method allows for control over the experimental conditions at the expense of using a foreign gas that is not of the same composition as Earth's atmosphere. Other studies have been performed using atmospheric air [11,16–18], however these studies lack control of the experimental parameters and are often performed at remote high altitude locations.

The present work is one of the few to be performed under laboratory conditions using dry air. This method provides for both control over the experimental parameters as well as a broadening gas with the same composition of the atmosphere. The experimental data between 0.3–1.5 THz were taken over multiple path lengths and humidity levels and were used to determine the total absorption coefficient of atmospheric air. Using these results coupled with calculated absorption coefficient values using the parameters in the 2008 HITRAN Database (HITRAN) [19], the foreign continuum coefficient for air was calculated and compared with other experimental data in the frequency region.

2. Experimental setup

Transmission data were collected using a Pike Technologies variable path length gas cell coupled to a Bruker Vertex 80 V Fourier Transform Infrared (FTIR) Spectrometer. A mercury arc lamp was used as the incident radiation source and the transmitted radiation was detected using a liquid He cooled silicon bolometer from IR Labs. In order to increase sensitivity the temperature of the bolometer was further reduced to 1.6 K by use of a vacuum pump. The cell was secured vertically in the sample chamber of the FTIR with the top protruding out. The FTIR's sample chamber was covered to allow the chamber to be purged with nitrogen gas to decrease atmospheric absorption from the optical path external to the cell. For the same reason, the FTIR's interferometer compartment, which is isolated from the sample chamber by polyethylene windows, was evacuated to below 1.5 Torr.

Fig. 1 shows the schematic of the absorption cell. The cell is able to achieve 1–16 m path lengths in 1 m increments. A micrometer at the top of the cell was used to adjust between different path lengths without a need to realign the setup. The cell was equipped with a Honeywell HIH-4000 relative humidity sensor and two Swagelok valves. One valve was connected to a vacuum pump for evacuating the cell while the second was connected to external sample containers. The pressure inside the cell was monitored using two capacitance manometer pressure sensors from MKS Industries. The sensors allowed for measurements ranging from 1000 Torr down to 10 mTorr.

Prior to the measurements the cell was evacuated to below 10 mTorr and then sealed. Background scans were completed for path lengths of 1–6 m consecutively. The distilled water vapor was then introduced into the cell, allowing adequate time for the pressure sensors to equalize. Following this, dry air purchased from Airgas East was introduced into the cell bringing the total pressure inside the cell to approximately 760 Torr. Finally sample scans with path lengths ranging from 1 to 6 m were completed.

The spectral region of interest was 300–1500 GHz and the spectral resolution of the FTIR was 3 GHz. The setup was optimized for this region by employing a 125 μm Mylar beamsplitter in the FTIR as well as a cold filter on the bolometer that attenuated any radiation with a frequency higher than 1500 GHz. A total of 6 transmission scans were collected at four relative humidity levels giving a total of 24 datasets. Relative humidity levels of 17.89%, 36.79%, 48.03%, and 70.84% were used. The partial pressure

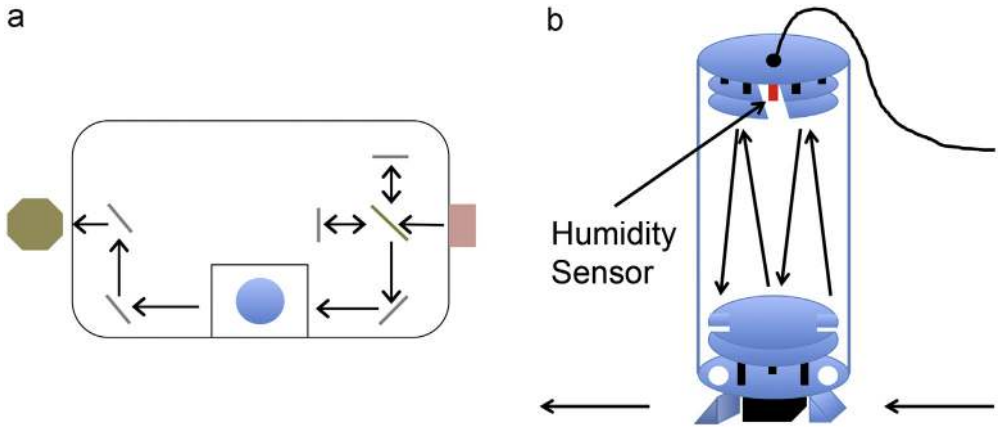

Fig. 1. A schematic of the setup used in the experiment is shown in (a). A diagram of the white cell used with the addition of the humidity sensor shown in red is displayed in (b). (For interpretation of the references to color in this figure legend, the reader is referred to the web version of this article.)

Please cite this article as: Slocum DM, et al. Atmospheric absorption of terahertz radiation and water vapor continuum effects. J Quant Spectrosc Radiat Transfer (2013), http://dx.doi.org/10.1016/j.jqsrt.2013.04.022

of water corresponding to these humidity levels was 3.60, 8.04, 10.05, and 15.23 Torr correspondingly. The laboratory temperature was 296 K for each dataset. Table 1 shows the parameters used on the Bruker Vertex 80 V FTIR for data collection.

Data was also collected in a narrow band centered at 1.560 THz using two separate measurement techniques. The first method used a Fabry–Perot resonator at the operating frequency. The absorption coefficient can be determined from a comparison of the resonator's loaded and unloaded quality factor, Q_l and Q_0 respectively, as shown in the following equation [20,21]:

$$\alpha = \frac{2\pi\nu}{c}\left(\frac{1}{Q_l} - \frac{1}{Q_0}\right) \tag{1}$$

An optically pumped molecular gas laser similar to that described in Ref. [22] was used as the frequency source.

Table 1
The parameters used on the Bruker FTIR.

Apodization function	Blackman–Harris 3 term
Internal aperture	8 mm
Non-linearity correction	0
Phase correction mode	Mertz
Phase resolution	4
Resolution	0.1 cm^{-1} (2997.92458 MHz)
Scanner velocity	80 kHz
Zero filling factor	1

The second method was an attenuation measurement performed in a compact radar range at the operating frequency after propagation through 25.9 m of open atmosphere in a climate controlled laboratory. The data for this measurement technique was collected over a one year period, which produced a range of relative humidity values from 10% to 50%. A detailed description of the experimental setup used for this technique can be found in Ref. [22].

3. Absorption coefficient measurements

Measurement of the absorption coefficient is done by use of the Beer–Lambert Law given in the following equation:

$$\tau = exp(-\alpha l) \tag{2}$$

The normalized transmission is shown as τ, α is the absorption coefficient, and l is the path length of the cell. Transmission spectra are taken at path lengths varying from 1 to 6 m and a straight line fit is performed at each frequency point using the natural log of the data as shown below:

$$\alpha l = -\ln(\tau) \tag{3}$$

The slope of the straight line in Eq. (3) gives the value of α. Fig. 2 shows as an example the measurement of α where the best fit straight line is displayed with the experimental data points. This procedure is repeated at all frequencies and humidity levels.

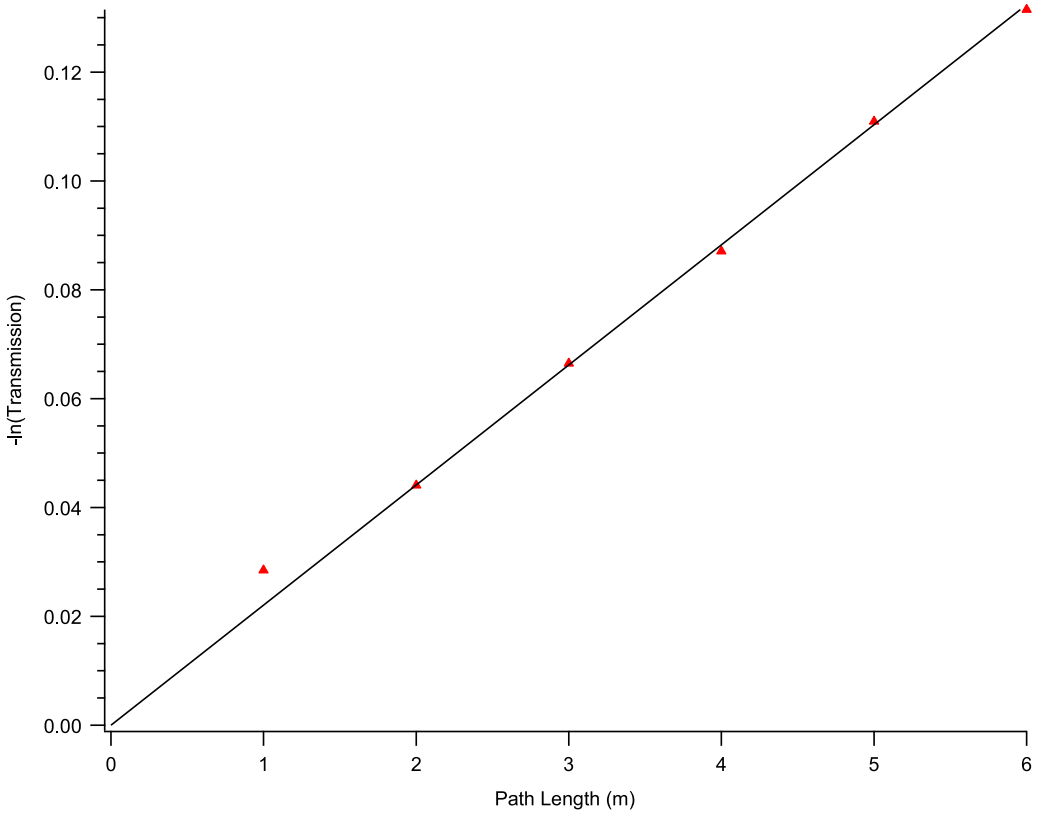

Fig. 2. A semi-log plot of transmission vs. path length for the 48.03% relative humidity data set at 862.224126 GHz. The markers are the experimental data while the solid line is the best fit approximation to the data.

Please cite this article as: Slocum DM, et al. Atmospheric absorption of terahertz radiation and water vapor continuum effects. J Quant Spectrosc Radiat Transfer (2013), http://dx.doi.org/10.1016/j.jqsrt.2013.04.022

4. Absorption coefficient calculations

Absorption coefficient calculations were performed at the humidity levels observed throughout the study. However, there was a discrepancy between two independent measurements of the partial pressure of water vapor inside the cell. The two values obtained were from pressure sensors recording the partial pressure of water vapor released into the cell and from the calculated partial pressure of water vapor determined from the output of the relative humidity sensor within the cell. This discrepancy was expected due to the process of adsorption of the water vapor to surfaces inside the cell and has been observed by other authors [9,23,24]. The effect of adsorption onto the optics has been previously investigated by other authors and was found to not affect the measurements for adsorbed layer thicknesses much less than the wavelength [24,25]. Therefore, the partial pressure of water vapor for this study is calculated from the humidity sensor reading. Comparison of the simulated and experimental spectra confirmed this effect. The simulated spectra for the partial pressure of water vapor released into the cell resulted in overestimated absorption peak amplitudes while the absorption peak amplitudes as determined from the output of the humidity sensor resulted in very good agreement with the experimental spectra.

4.1. Water vapor absorption line simulation

Each of the water vapor absorption lines were calculated using parameters from HITRAN as well as the Van Vleck-Weisskopf line shape function given below [26]:

$$\alpha_k(\nu) = \alpha_{k,max}\frac{\nu}{\nu_k}\left[\frac{1}{((\nu-\nu_k)/\Delta\nu_k)^2+1}+\frac{1}{((\nu+\nu_k)/\Delta\nu_k)^2+1}\right] \tag{4}$$

In Eq. (4), $\alpha_{k,\max}$ is the amplitude of the self broadened absorption line in units of m^{-1} and ν, ν_k, and $\Delta\nu_k$ are the frequency of the incident radiation, line center frequency, and line half width respectively in MHz. No line cut off frequency was used and a high frequency limit of 2.1 THz was employed, corresponding to 750 GHz beyond the final data point.

The half width was calculated as follows:

$$\Delta\nu_k = \gamma_{ks}P_s + \gamma_{kf}P_f \tag{5}$$

The amplitude of the line shape was calculated using Eq. (6), which is from Ref [27]:

$$\alpha_{k,max} = \frac{I_k}{\gamma_{ks}}10,245.8 \tag{6}$$

In Eqs. (5) and (6) γ_{ks} and γ_{kf} are the self and foreign gas line broadening coefficients in MHz/Torr, P_s and P_f are the partial pressures of water vapor and air respectively in Torr, I_k is the line intensity in units of nm^2 MHz, and the constant in Eq. (6) is a unit conversion factor.

The simulation of a single water vapor absorption line is performed in two steps. In step 1, the self-broadened line shape is calculated using Eqs. (4)–(6) and the partial pressure of water vapor. In step 2, the effects of foreign gas broadening are calculated using the partial pressure of dry air while maintaining the integrated line strength determined from step 1. The observed partial pressures of water vapor were large enough that only pressure broadening

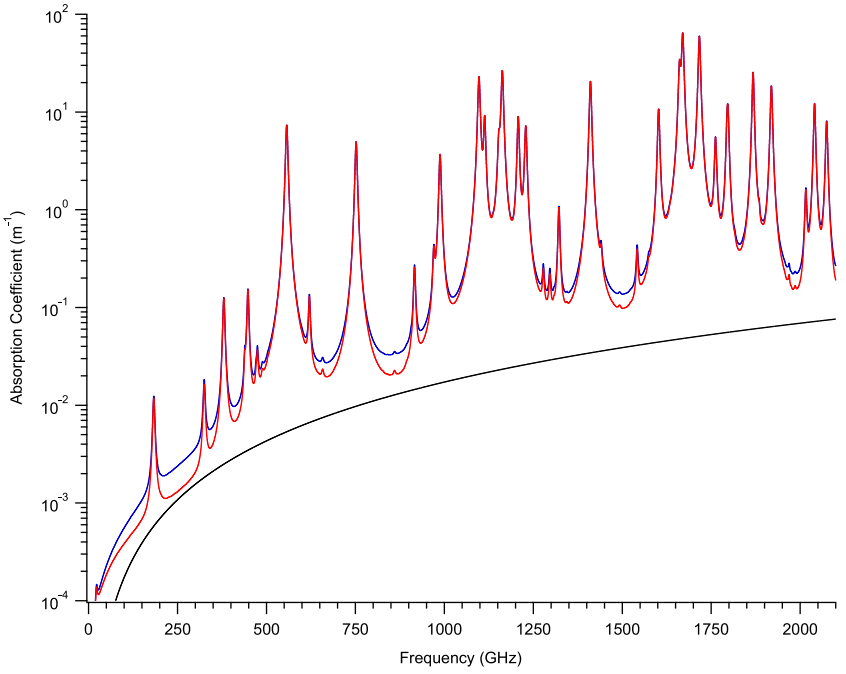

Fig. 3. The calculated air-broadened spectrum (red), continuum absorption (black), and air-broadened spectrum with continuum absorption (blue). All plots are 15.23 Torr of water vapor and 746.77 Torr of air. (For interpretation of the references to color in this figure legend, the reader is referred to the web version of this article.)

Please cite this article as: Slocum DM, et al. Atmospheric absorption of terahertz radiation and water vapor continuum effects. J Quant Spectrosc Radiat Transfer (2013), http://dx.doi.org/10.1016/j.jqsrt.2013.04.022

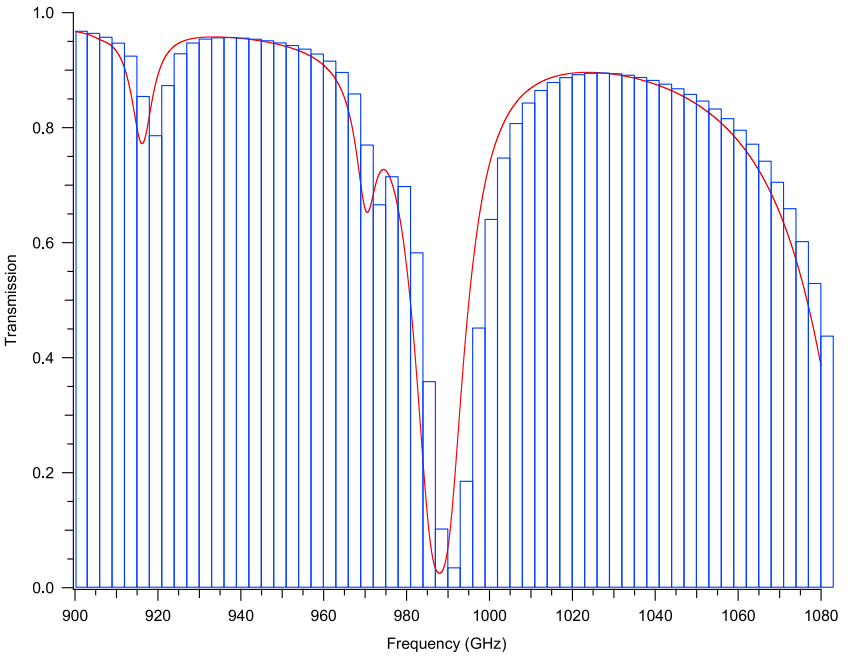

Fig. 4. A section of the calculated transmission spectrum of 15.23 Torr of water vapor and 746.77 Torr of air (red) and the same spectrum after calculated instrumentation distortion has been applied, shown with the resolution bins (blue). (For interpretation of the references to color in this figure legend, the reader is referred to the web version of this article.)

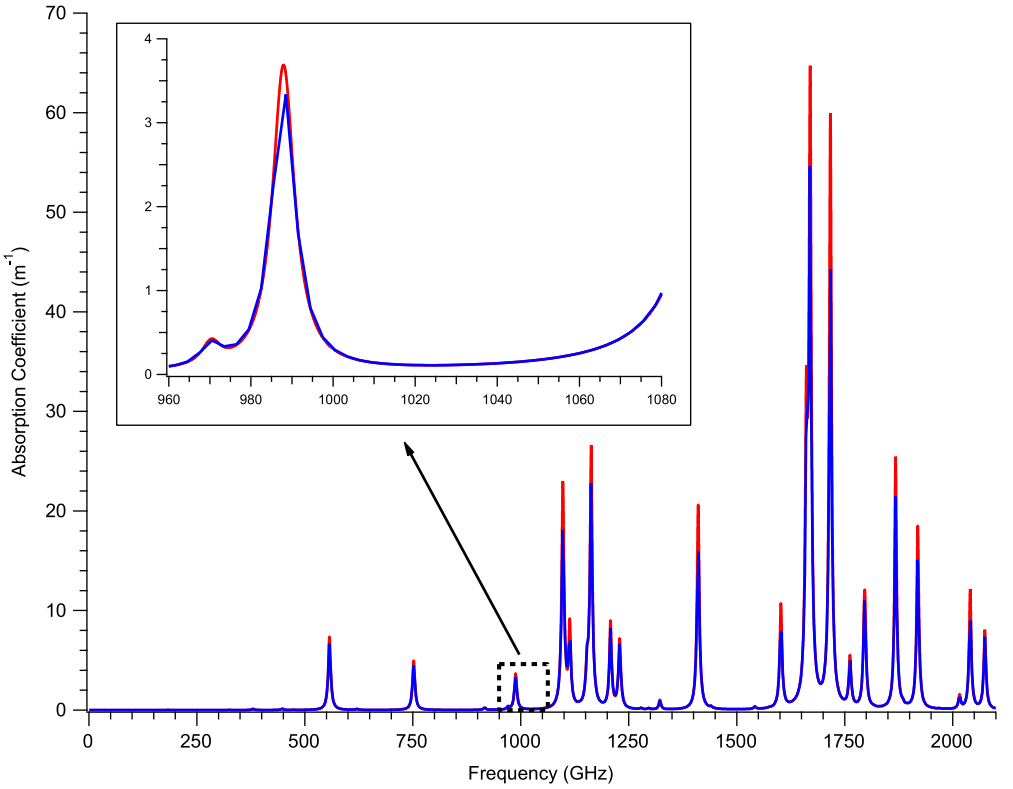

Fig. 5. The calculated air-broadened absorption coefficient for 15.23 Torr of water vapor and 746.77 Torr of air (red) and the same spectrum after applying the calculated instrumentation distortion (blue). (For interpretation of the references to color in this figure legend, the reader is referred to the web version of this article.)

Please cite this article as: Slocum DM, et al. Atmospheric absorption of terahertz radiation and water vapor continuum effects. J Quant Spectrosc Radiat Transfer (2013), http://dx.doi.org/10.1016/j.jqsrt.2013.04.022

and not Doppler broadening need be considered. Within this regime the Van Vleck-Weisskopf line shape, Eq. (4), is the appropriate line shape choice [28].

4.2. Water vapor absorption spectrum simulation

In order to obtain the full water vapor absorption spectrum, each individual water vapor line in HITRAN within the studied frequency region was calculated utilizing the process described in Section 4.1. Each foreign gas broadened absorption line was summed according to Eq. (7) to form the absorption coefficient as a function of frequency.

$$\alpha_l(\nu) = \sum_k \alpha_k(\nu) \tag{7}$$

In Eq. (7) the absorption coefficient due to all of the resonant water vapor absorption lines is shown as α_l in units of m^{-1}. Fig. 3 shows the resonant line simulation for 15.23 Torr of water vapor and 746.77 Torr of air corresponding to a relative humidity of 70.84%.

4.3. Continuum absorption simulation

In order to accurately model the total observed absorption coefficient, continuum absorption must be accounted for. The water vapor continuum can be calculated using [8–10,13,14]

$$\alpha_c(\nu) = \nu^2 P_s(P_s C_s \theta^{n_s} + P_f C_f \theta^{n_f}) \tag{8}$$

In Eq. (8) α_c is the continuum contribution to the absorption coefficient, C_s and C_f are the self and foreign continuum coefficients in units of $m^{-1}/(Torr^2\,MHz^2)$, the exponential terms n_s and n_f are the self and foreign temperature exponents, and θ is a reference temperature of 300 K divided by the gas temperature in Kelvin. The continuum absorption calculated from Eq. (8) is then added to the air-broadened absorption spectrum from the previous section. Fig. 3 shows the effects of the continuum added to the water vapor spectrum. Note that the continuum has a small but measureable effect on the absorption coefficient.

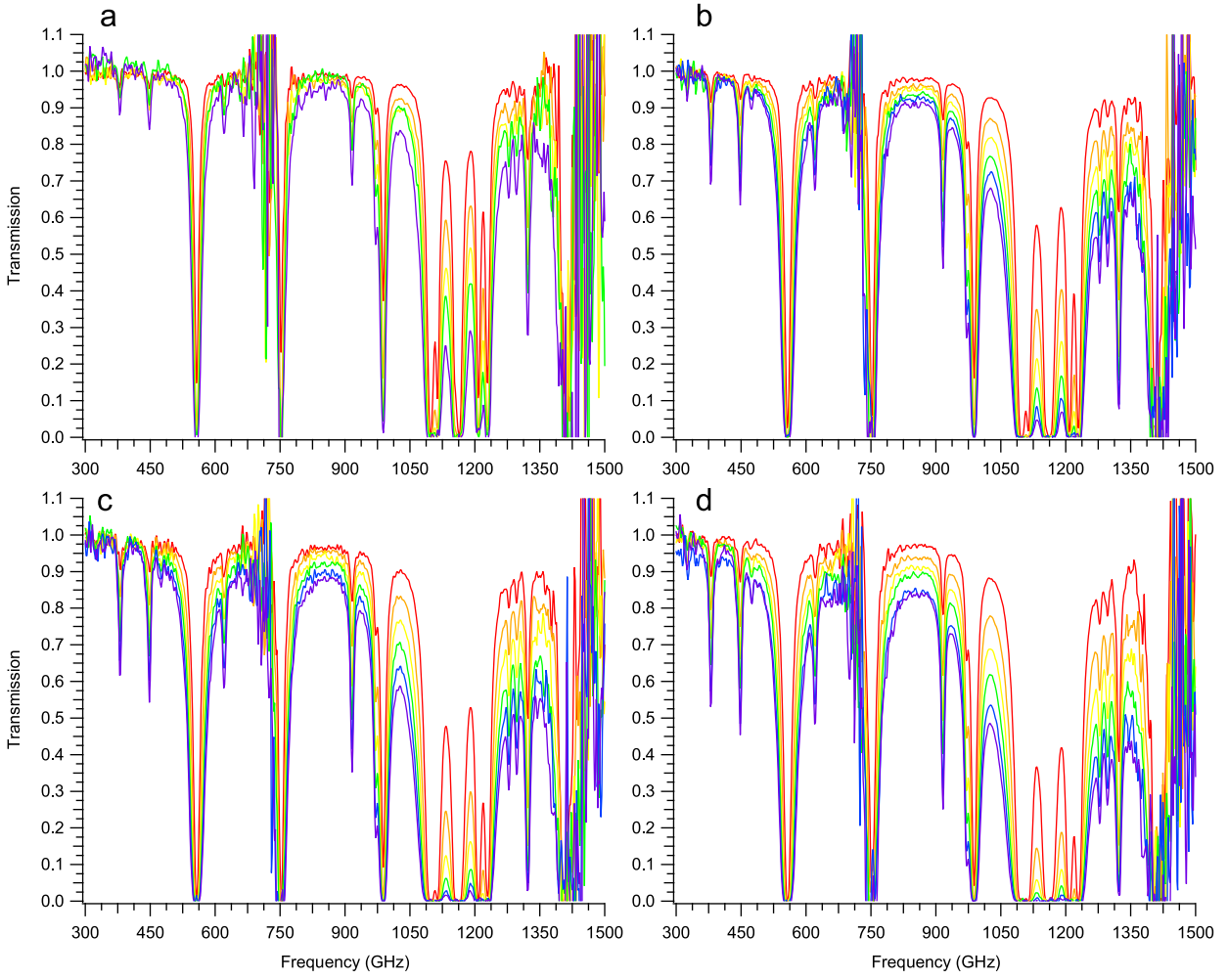

Fig. 6. Plots of transmission vs. frequency for 17.89%, 36.78%, 48.03%, and 70.84% relative humidity for (a)–(d) correspondingly. The path lengths depicted are 1–6 m for the red, orange, yellow, green, blue and purple traces correspondingly. The effects of the beamsplitter null and cold filter are seen at 0.73 and 1.50 THz respectively. (For interpretation of the references to color in this figure legend, the reader is referred to the web version of this article.)

Please cite this article as: Slocum DM, et al. Atmospheric absorption of terahertz radiation and water vapor continuum effects. J Quant Spectrosc Radiat Transfer (2013), http://dx.doi.org/10.1016/j.jqsrt.2013.04.022

4.4. Instrumentation distortion simulation

The discrete nature of the experimental apparatus imposed a distortion on the otherwise continuously varying structure of the absorption spectra. The FTIR uses discrete resolution bins in the Fast Fourier Transform of the transmission spectra. In order to accurately model the distortion, the calculated absorption spectra are transformed into transmission spectra using the Beer–Lambert-Law, Eq. (2), and a fixed path length of 1 m. The predicted power absorbed in each frequency bin of the FTIR was then calculated. Fig. 4 shows a section of a transmission spectrum with the effective resolution bins overlaid. Once the distortion was accounted for, the transmission spectra were transformed back into absorption coefficient space. Finally, for comparison with the measured spectra, the calculated spectra were interpolated. The calculated discrete frequency points were forced to the same values as the measured spectra through the use of a linear interpolation of the absorption coefficient values. Fig. 5 shows a calculated spectrum, without continuum absorption, and the same spectrum after the instrumentation distortion has been applied. Note that the instrumentation distortion lowers the peak value of the spectral line and broadens it from the undistorted spectra. This effect is more pronounced for data sets with lower resolution but must still be taken into account for the measurements in this work.

5. Results

Displayed in Fig. 6 are the transmission spectra as recorded by the FTIR. The plots show the transmission of terahertz radiation through air at relative humidity levels of 17.89%, 36.78%, 48.03%, and 70.84% for path lengths of 1–6 m. The 5 m path length data has been removed from the 17.89% relative humidity dataset because the background scan proved to be unstable. The transmission plots show regions of significant noise at 300, 750, and 1500 GHz due to a low amount of power in the measurements. The cause is from the source, a beamsplitter null, and attenuation from the bolometer cold filter at the low end, center, and high end of the studied frequency region respectively. Saturation effects can also be noticed in many of the strong absorption lines, in particular in the 1.050–1.250 THz range.

Using the transmission spectra, the absorption coefficient was determined according to the process outlined in Section 3. Plots of the experimental absorption coefficient

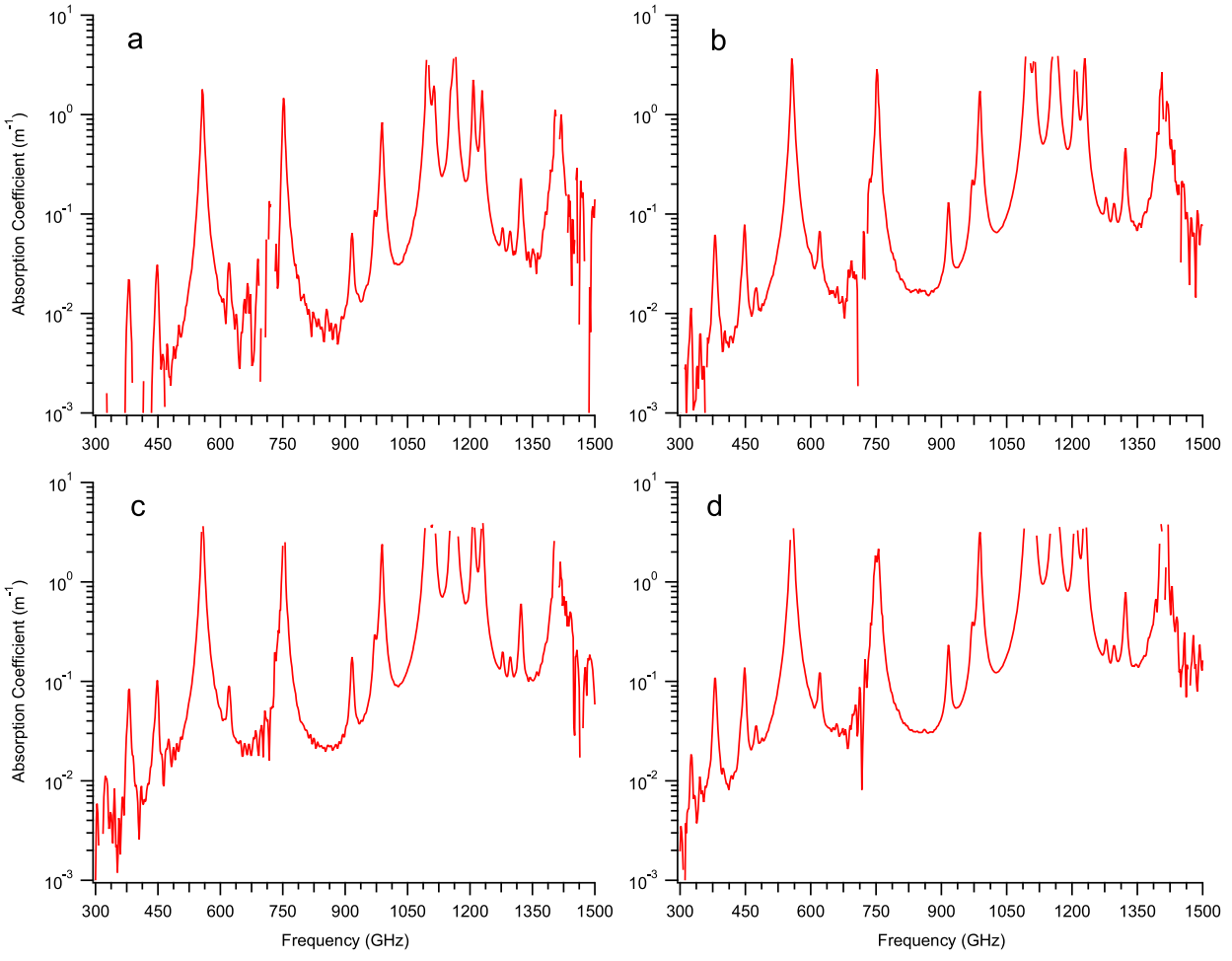

Fig. 7. Plots of experimental absorption coefficient vs. frequency for 17.89%, 36.78%, 48.03%, and 70.84% relative humidity for (a)–(d) correspondingly.

Please cite this article as: Slocum DM, et al. Atmospheric absorption of terahertz radiation and water vapor continuum effects. J Quant Spectrosc Radiat Transfer (2013), http://dx.doi.org/10.1016/j.jqsrt.2013.04.022

for the observed relative humidity levels can be seen in Fig. 7. The missing data from the plotted absorption lines are due to saturation. The calculation of the absorption coefficient from the transmission spectra is limited to values less than 4 m^{-1} due to saturation effects. It is also important to note that the 752 GHz line falls within the beamsplitter null and cannot be used for comparison and observations. The statistical error for each data point was calculated from the fitting routine of the absorption coefficient. The average error across the data range, excluding regions of low signal to noise, was 8.85%, 4.00%, 3.67%, and 2.87% for the 17.89%, 36.78%, 48.03%, and 70.84% relative humidity datasets respectively.

Table 2
A table of the water vapor absorption line data from HITRAN for the observed lines in the FTS measurements from the present study.

Frequency (GHz)	Lower state energy (cm^{-1})	Intensity (nm^2 MHz)	Upper quantum numbers	Lower quantum numbers
380	212	2.49E−03	$4_{1,4}$	$3_{2,1}$
448	285	2.60E−03	$4_{2,3}$	$3_{3,0}$
557	24	1.58E−01	$1_{1,0}$	$1_{0,1}$
621	488	1.71E−03	$5_{3,2}$	$4_{4,1}$
916	285	4.30E−03	$4_{2,2}$	$3_{3,1}$
970	384	4.82E−03	$5_{2,4}$	$4_{3,1}$
988	37	7.59E−02	$2_{0,2}$	$1_{1,1}$
1097	137	4.93E−01	$3_{1,2}$	$3_{0,3}$
1113	0	1.51E−01	$1_{1,1}$	$0_{0,0}$
1163	173	5.38E−01	$3_{2,1}$	$3_{1,2}$
1208	275	1.67E−01	$4_{2,2}$	$4_{1,3}$
1229	95	1.45E−01	$2_{2,0}$	$2_{1,1}$
1278	889	2.14E−03	$7_{4,3}$	$6_{5,2}$
1296	842	2.07E−03	$8_{2,7}$	$7_{3,4}$
1322	509	1.71E−02	$6_{2,5}$	$5_{3,2}$

The experimental absorption coefficient data was used to determine the air-broadened continuum coefficient. The calculated absorption coefficient spectra without a continuum contribution were subtracted from the experimental spectra to yield the empirical continuum absorption data. Eq. (8) was then fit to these spectra using $C_f^* = C_f \theta^{n_f}$ as the fitting parameter. All of the data from the present study were obtained at 296 K so the θ^{n_f} term is a multiplicative constant for the present study. The value of $C_f^* = 1.158 \times 10^{-18}$ $m^{-1}/(Torr^2\,MHz^2)$ was found to minimize the mean square error of all four humidity levels. The resolution of the spectrometer was too large to be able to resolve any self-broadened absorption peak of water vapor and hence self-broadening data was not taken. It was therefore only possible to determine one of the continuum coefficients. The air-broadened continuum coefficient was investigated in this study because air, and not nitrogen, was used as a broadening gas for this study. The value for C_s^* that provided the smallest error was from Podobedov et al. [13,14].

Fifteen of the strongest water vapor absorption lines were identified in the spectra and were compared with

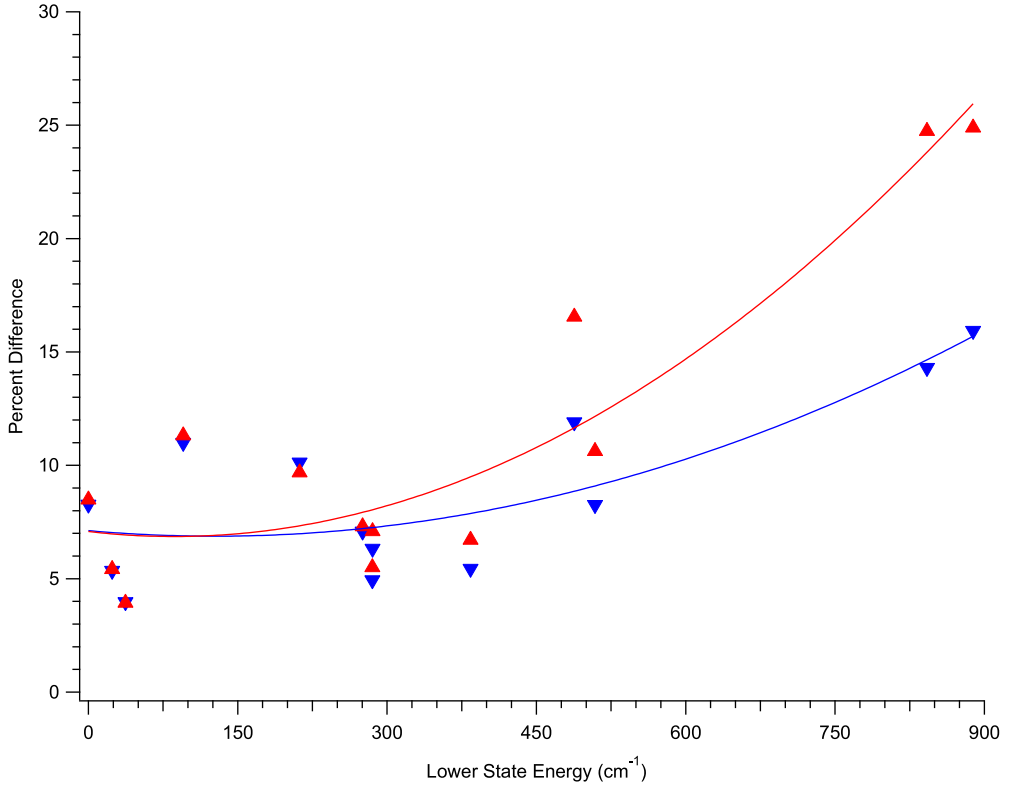

Fig. 8. Plots of the percent difference in the amplitude of the water vapor absorption lines versus the lower state energy of the absorption line for both with (blue) and without (red) continuum absorption. The markers are the experimental data while the solid lines are a quadratic fit to the data. (For interpretation of the references to color in this figure legend, the reader is referred to the web version of this article.)

Please cite this article as: Slocum DM, et al. Atmospheric absorption of terahertz radiation and water vapor continuum effects. J Quant Spectrosc Radiat Transfer (2013), http://dx.doi.org/10.1016/j.jqsrt.2013.04.022

values from HITRAN and the Jet Propulsion Laboratory Database (JPL) [27]. All of the measured absorption peak locations were in agreement with HITRAN and JPL within the experimental uncertainty. Some of the available line parameters from HITRAN of the observed lines are shown in Table 2.

Fig. 8 shows a plot of the average percent difference of the absorption peak amplitudes between the observed and calculated spectra for the FTS measurements. The percent difference is averaged over the humidity values and is plotted against the absorption line lower state energy. A noticeable trend of increasing discrepancy with increasing lower state energy can be seen in the plot. The percent difference is lower when the calculated spectrum includes a continuum contribution and the trend of increasing discrepancy at larger lower state energies is shallower.

The percent difference was also plotted against the absorption line frequency, however there was no clear trend in the data between the percent difference and the frequency of the line. The resonant line absorption coefficient model as well as the continuum absorption model used in the calculations takes into account the frequency

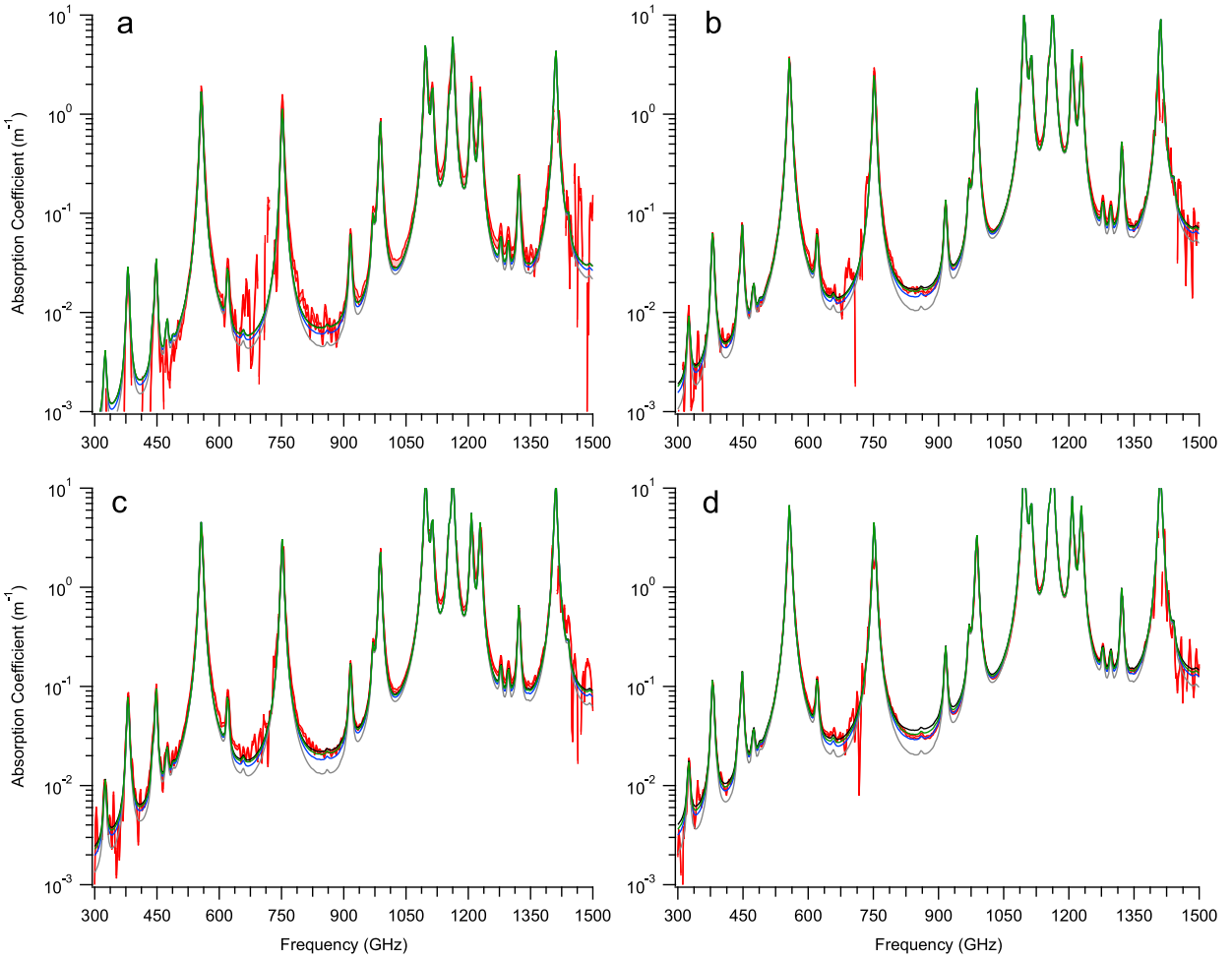

Fig. 9. Absorption spectra of 17.89%, 36.78%, 48.03%, and 70.84% relative humidity for plots (a)–(d) correspondingly. Shown on each plot is the experimental (red), resonant line simulation (gray), and the resonant line simulation with continuum absorption for the Kuhn et al., Podobedov et al., and present study continuum parameter sets in black, blue, and green respectively. (For interpretation of the references to color in this figure legend, the reader is referred to the web version of this article.)

Table 3
The continuum parameters used throughout the study. The continuum coefficients C_s and C_f are given in units of $m^{-1}/(Torr^2\ MHz^2)$.

Parameter set	C_s	C_f	n_s	n_f
Kuhn et al. [9]	3.637e−17	1.030e−18	8.289	4.551
Podobedov et al. [13,14]	1.57e−17	6.5e−19	8.8	5.5
Present study	$(1.76e{-}17^{a})/\theta^{n_s}$	$(1.158e{-}18)/\theta^{n_f}$	NA	NA

[a]The value for C_s was taken from Podobedov et al. [13,14].

Please cite this article as: Slocum DM, et al. Atmospheric absorption of terahertz radiation and water vapor continuum effects. J Quant Spectrosc Radiat Transfer (2013), http://dx.doi.org/10.1016/j.jqsrt.2013.04.022

dependence, therefore the fact that there was no trend between the percent difference and the frequency was expected.

6. Comparisons

Fig. 9 shows the experimental absorption spectra compared with the calculated absorption spectra. The calculated spectra have been calculated using the procedure outlined in Section 4 with HITRAN as an input. The continuum contributions were calculated using several different parameter sets. The different continuum parameter sets used throughout the study are presented in Table 3. As can be seen in Fig. 9, the predicted and measured spectra in general show very good agreement. However, no set of continuum parameters is able to exactly model the experimental spectra across the whole frequency region for all datasets. It is necessary to account for continuum absorption in the calculated spectra and all three parameter sets provide reasonable agreement with the observed spectra. The most pronounced example for the need of the continuum is at 850 GHz where the spectrum calculated without the continuum shows a large difference from the experimental results.

Figs. 10 and 11 show an expanded view of the atmospheric windows centered at 0.87 and 1.30 THz. In all but the highest relative humidity dataset the calculated spectra predict less total absorption than is experimentally observed in the 1.3 THz window. If the continuum absorption were increased however, the prediction would overestimate the total absorption in the 870 GHz window. The cause of the less accurate predictions in the 1.3 THz window is more likely from the large absorption lines immediately adjacent to the window. If the calculated pressure-broadening parameters for these lines were underestimated, this could account for the difference between the observed and calculated spectra in this region. The broadening of these absorption lines would raise the absorption coefficient spectrum in the region

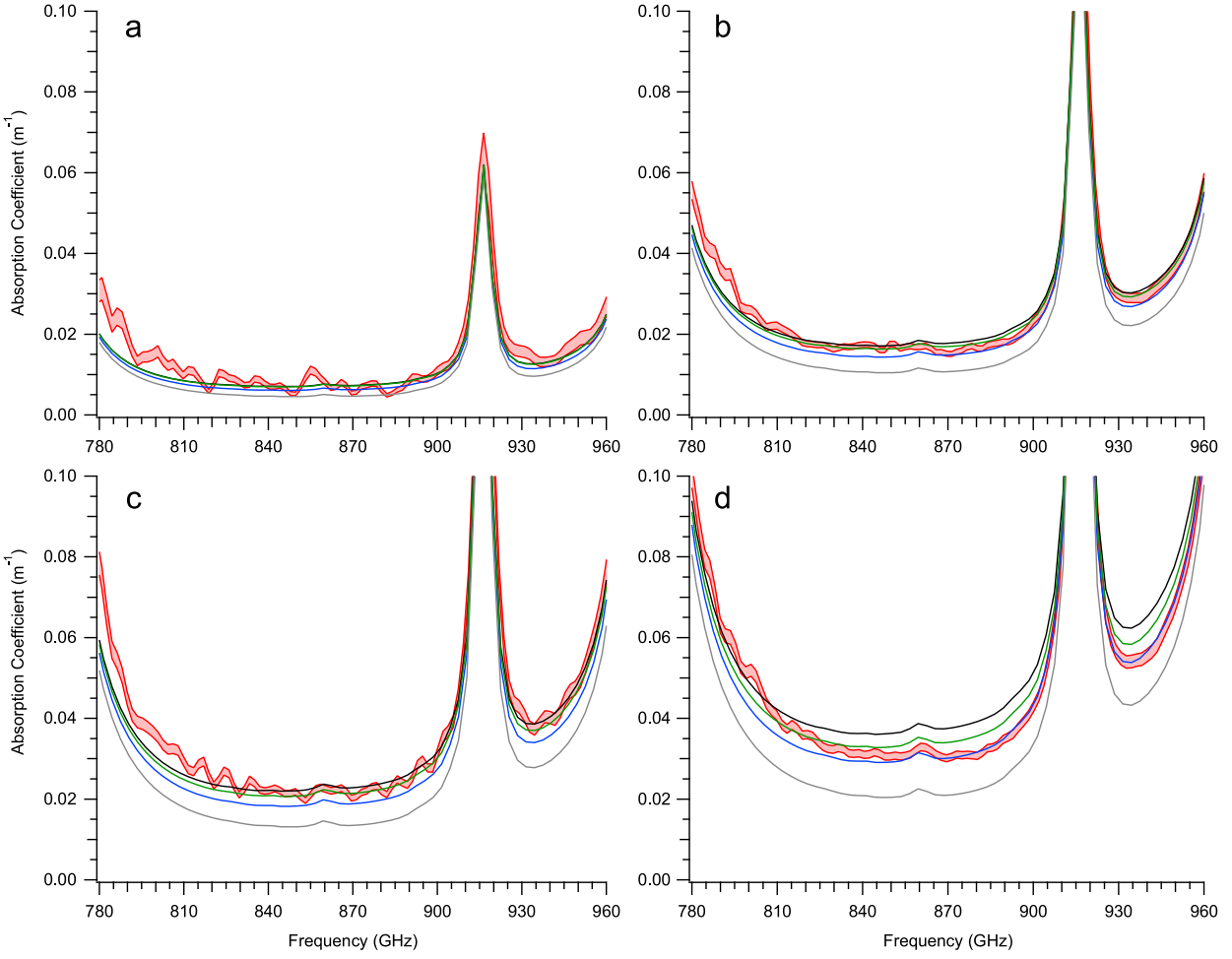

Fig. 10. Comparison of the total absorption coefficient in the transmission window centered at 870 GHz. Plotted are the upper and lower statistical bounds of the experimental spectra (red), the resonant line simulation (gray), and the resonant line simulation with continuum absorption for the Kuhn et al., Podobedov et al., and present study continuum parameter sets in black, blue, and green respectively. Plots are shown for 17.89%, 36.78%, 48.03%, and 70.84% relative humidity in (a)–(d) correspondingly. (For interpretation of the references to color in this figure legend, the reader is referred to the web version of this article.)

Please cite this article as: Slocum DM, et al. Atmospheric absorption of terahertz radiation and water vapor continuum effects. J Quant Spectrosc Radiat Transfer (2013), http://dx.doi.org/10.1016/j.jqsrt.2013.04.022

immediately around the line while lowering the peak amplitude of the line. The effect on the rest of the spectrum, far enough removed from the absorption line, would be minimal.

The percent difference between the experimental and calculated spectra was studied to determine which continuum parameter set provides the best match to the observed spectra. The data used for this determination are from the window regions centered at 400, 870, 1025, and 1300 GHz with outliers due to low signal to noise areas removed. It is clear from this data and Figs. 9–11 that all three continuum parameter sets result in a better match to the experimental spectra than no continuum set. However, the parameter set that provides the best agreement with the experimental data is from the present study since the constant C_f has been fit to minimize the mean square error.

The two continuum parameter sets from the literature used throughout this study were determined using older versions of HITRAN, the Podobedov et al. set used the 2004 version while the Kuhn et al. set used the 2000 version. Between the 2000 and 2004 versions self-broadening parameters were added to the database and between the 2004 and 2008 versions the air-broadening half widths were updated. The use of a different line parameter database would yield a different result for the resonant line spectrum and hence the calculated empirical continuum absorption. These differences, however, only effect the continuum contribution to the calculated absorption coefficient in this study. After comparison of the resulting spectra from the three continuum parameter sets with each other and the experimental spectra, the use of different versions of the HITRAN database did not produce significant differences.

Fig. 12 shows a correlation plot of experimental data and values calculated according to the procedure outlined in Section 4. Displayed in the figure are the cavity Q data, the direct attenuation data, and the peak absorption line data of the FTS measurements from the present study. Also displayed in the figure are data points from cavity Q measurements

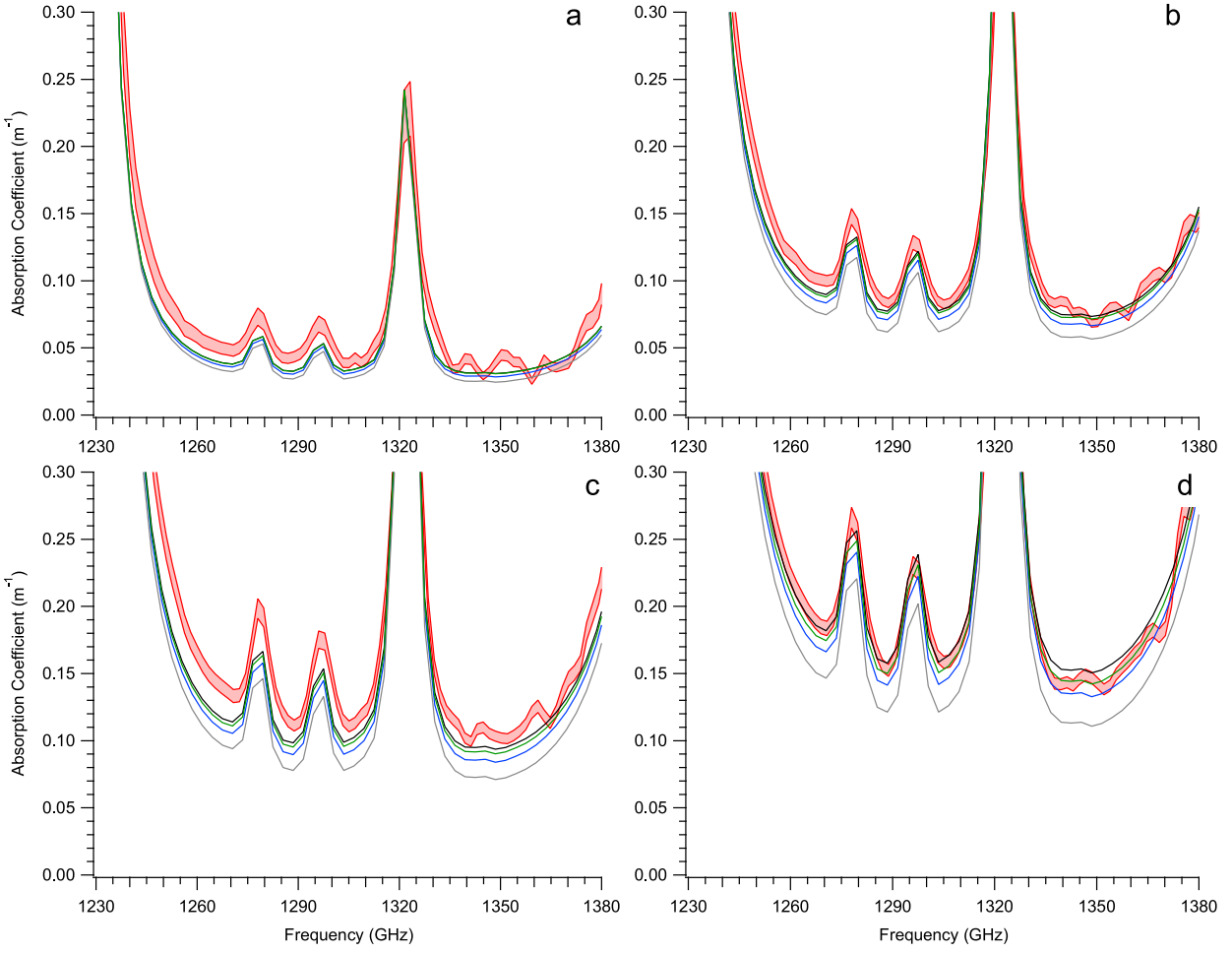

Fig. 11. Comparison of the total absorption coefficient in the transmission window centered at 1.3 THz. Plotted are the upper and lower statistical bound of the experimental spectra (red), the resonant line simulation (gray), and the resonant line simulation with continuum absorption for the Kuhn et al., Podobedov et al., and present study continuum parameter sets in black, blue, and green respectively. Plots are shown for 17.89%, 36.78%, 48.03%, and 70.84% relative humidity in (a)–(d) correspondingly. (For interpretation of the references to color in this figure legend, the reader is referred to the web version of this article.)

Please cite this article as: Slocum DM, et al. Atmospheric absorption of terahertz radiation and water vapor continuum effects. J Quant Spectrosc Radiat Transfer (2013), http://dx.doi.org/10.1016/j.jqsrt.2013.04.022

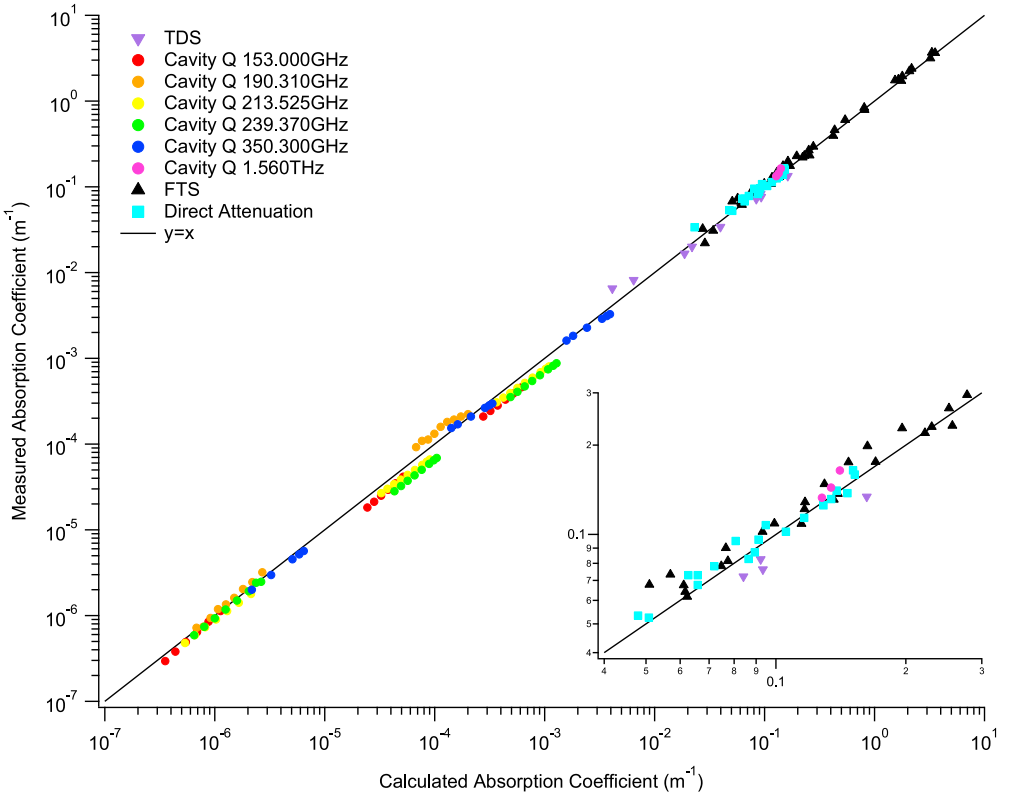

Fig. 12. Correlation plot for various experimental data and our model predictions. A straight line of unit slope is provided as a reference for 100% correlation.

Table 4
The results of the 1.560 THz absorption measurements performed for this work.

Relative humidity (%)	Measured absorption coefficient (m^{-1})	Predicted absorption coefficient (m^{-1})
10.1[a]	0.03378	0.02564
17[a]	0.05334	0.04910
17.8[a]	0.05245	0.05182
21.1[a]	0.07290	0.06304
22[a]	0.06757	0.06610
22[a]	0.07290	0.06610
23.7[a]	0.07823	0.07188
26.1[a]	0.09513	0.08004
27.7[a]	0.08268	0.08548
28.5[a]	0.08712	0.08820
29[a]	0.09602	0.08990
30[a]	0.1076	0.09330
33[a]	0.1022	0.1035
36[a]	0.1138	0.1137
39.5[a]	0.1254	0.1256
41[a]	0.1316	0.1307
42.1[a]	0.1405	0.1344
44[b]	0.1330	0.1241
44.4[a]	0.1378	0.1423
45.6[a]	0.1645	0.1463
46[a]	0.1591	0.1477
46[b]	0.1440	0.1301
48[b]	0.1644	0.1361

[a] Direct attenuation measurement.
[b] Cavity Q measurement.

obtained from Refs. [9,29–32] and Terahertz Time Domain Spectroscopy obtained from Ref. [33]. The calculation routine is able to accurately model from 1.5 THz down into the microwave region to at least 153 GHz for both self and foreign gas broadening at varying temperatures. The measurements performed in Refs. [9,29–32] were done at 1 Torr and 10 Torr partial pressure of water vapor at temperatures from 296 to 376 K for both self and foreign gas broadening. Four different measurement techniques across eight orders of magnitude in the absorption coefficient can also be accurately modeled using the calculations. Each measurement technique has a different instrumentation distortion, and this distortion must be accounted for an accurate comparison of any data. The present study accounted for the distortion in each spectrum according to the process outline in Section 4.4.

The results of the 1.560 THz absorption measurements from the present work are displayed in Table 4. These Cavity Q measurements were performed by flowing atmospheric air at 294 K through the cavity with a base path length of 2.438 m and the direct attenuation measurements were performed at 296 K with a path length of 25.9 m.

7. Absorption coefficient predictions

The process outlined in Section 4 was used to create a set of predictions of the total absorption coefficient of the

Please cite this article as: Slocum DM, et al. Atmospheric absorption of terahertz radiation and water vapor continuum effects. J Quant Spectrosc Radiat Transfer (2013), http://dx.doi.org/10.1016/j.jqsrt.2013.04.022

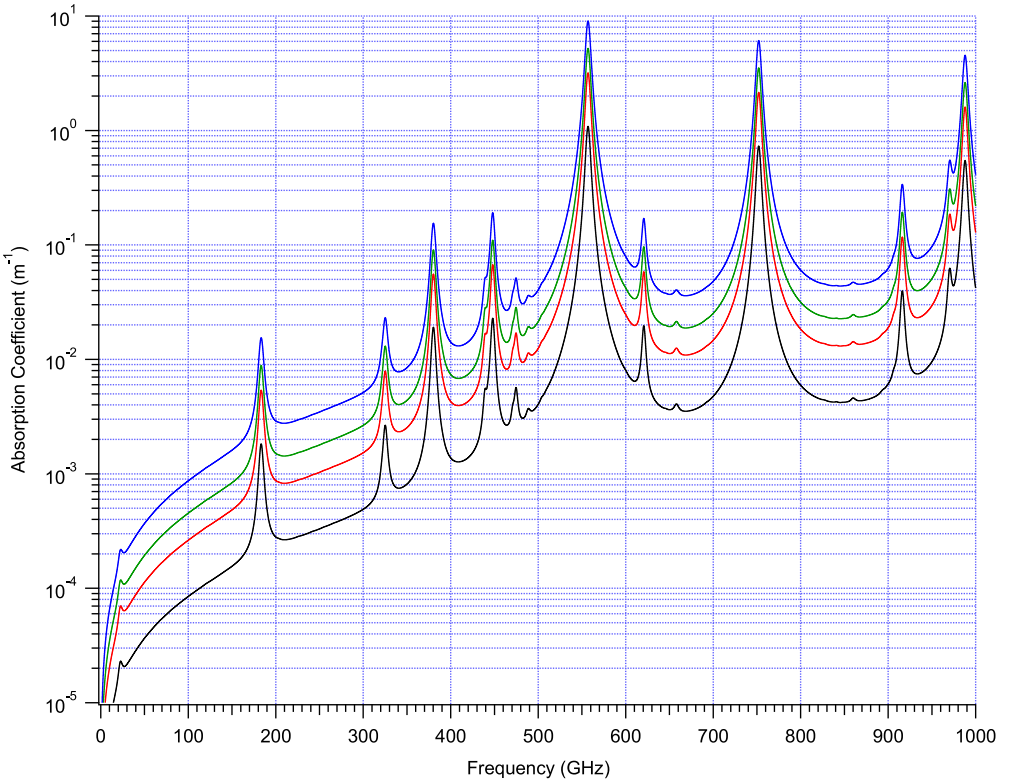

Fig. 13. A plot of the predicted absorption coefficient for relative humidity levels of 10–90% at 296 K for frequencies from 0 to 1 THz.

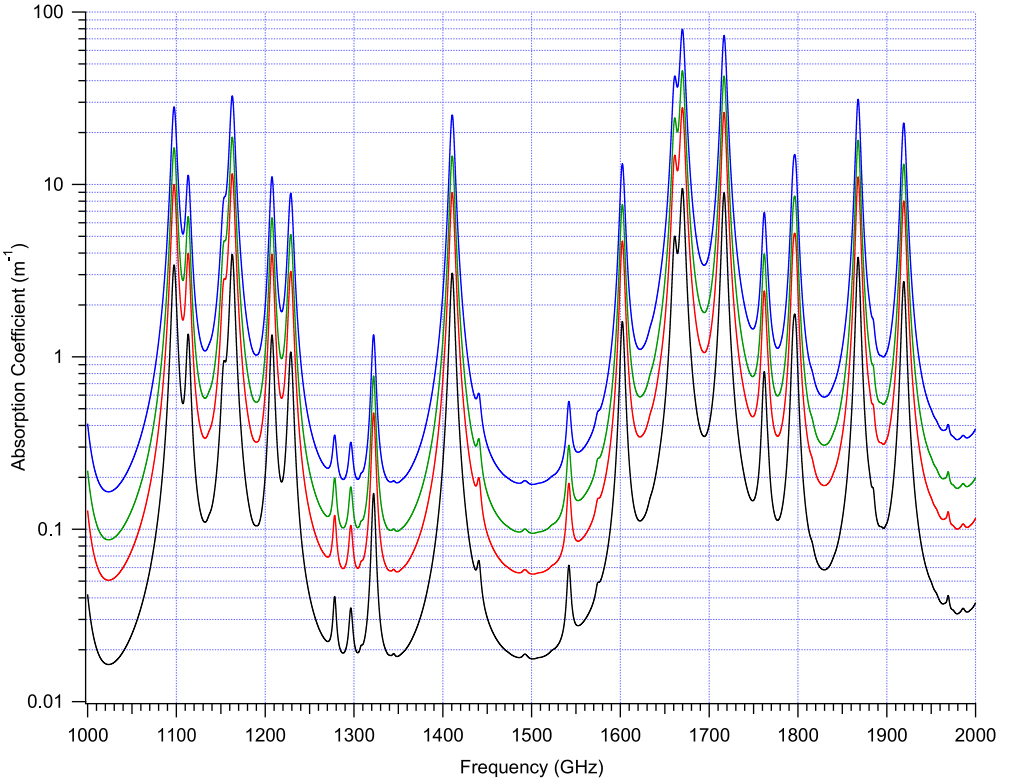

Fig. 14. A plot of the predicted absorption coefficient for relative humidity levels of 10–90% at 296 K for frequencies from 1 to 2 THz.

Please cite this article as: Slocum DM, et al. Atmospheric absorption of terahertz radiation and water vapor continuum effects. J Quant Spectrosc Radiat Transfer (2013), http://dx.doi.org/10.1016/j.jqsrt.2013.04.022

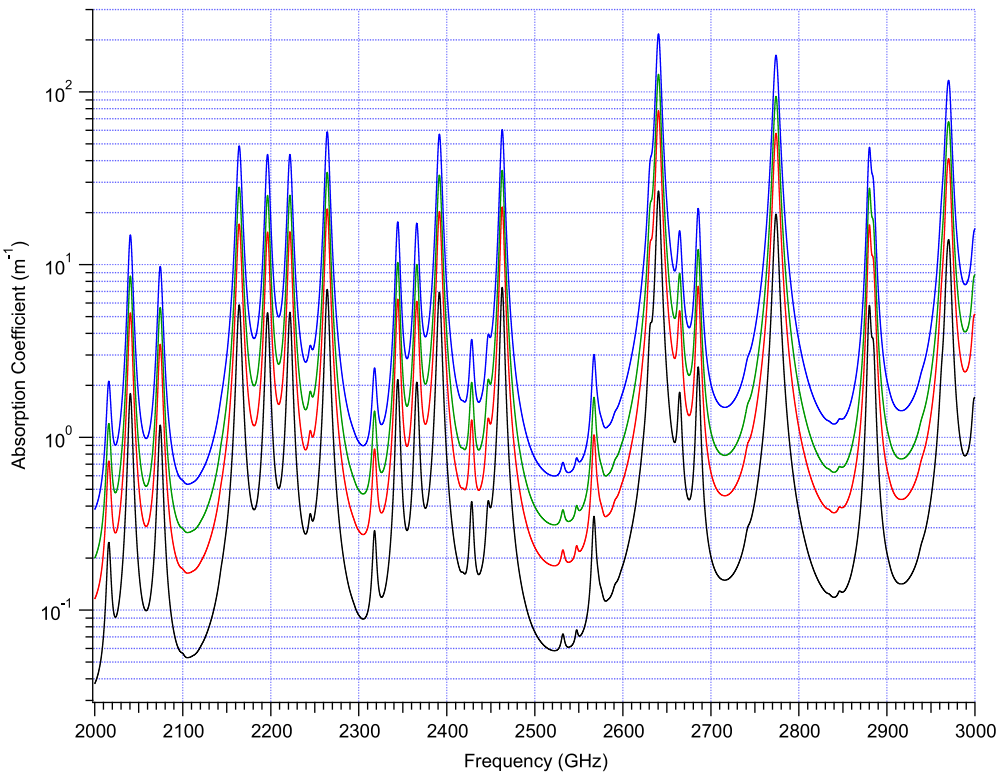

Fig. 15. A plot of the predicted absorption coefficient for relative humidity levels of 10–90% at 296 K for frequencies from 2 to 3 THz.

atmosphere for relative humidity levels ranging from 10% to 90% in increments of 10% for 0–3 THz at a temperature of 296 K. The predictions have accounted for continuum absorption using the parameter set from the present study. Plots of the absorption coefficient of air with a relative humidity of 10%, 30%, 50% and 90% can be seen in Figs. 13–15. Instrumentation distortion is not included in these calculations.

8. Conclusions

Broadband absorption measurements of water vapor dispersed in air were presented in the 0.300–1.500 THz region for varying relative humidity levels. The transmission spectra over multiple path lengths were recorded using FTS and the absorption coefficient as a function of frequency was calculated. Using a standard Van Vleck-Weisskopf line shape, the resonant line absorption spectra and the continuum absorption were calculated. Using the calculated continuum absorption, the air-broadened continuum coefficient for water vapor was determined and compared with available data from the literature. The present study calculated the air-broadened continuum coefficient to be 1.158×10^{-18} m^{-1}/(Torr^2 MHz^2), as much as 80% larger than other values found in the literature. This value however seems to be within the scatter of the values from previous measurements. The calculation routine was also used to simulate the total observed absorption by other authors. The calculated spectra provide good agreement with measurements across eight orders of magnitude in the absorption coefficient for multiple measurement techniques through a wide range of pressures and temperatures.

References

[1] Payne VH, Delamere JS, Cady-Pereira KE, Gamache RR, Moncet JL, Mlawer EJ, et al. Air-broadened half-widths of the 22- and 183-GHz water-vapor lines. IEEE Trans Geosci Remote Sens 2008;46:3601–17.
[2] Gamache RR, Laraia AL. N_2-, O_2-, and air-broadened half-widths, their temperature dependence, and line shifts for the rotational band of $H_2{}^{16}O$. J Mol Spectrosc 2009;257:116–27.
[3] Ma Q, Tipping RH, Gamache RR. Uncertainties associated with theoretically calculated N_2-broadened half-widths of H_2O lines. Mol Phys 2010;108:2225–52.
[4] Ma Q, Tipping RH. Water vapor continuum in the millimeter spectral region. J Chem Phys 1990;93:6127–39.
[5] Pardo JR, Cernicharo J, Serabyn E. Atmospheric Transmission at Microwaves (ATM): an improved model for millimeter/submillimeter applications. IEEE Trans Antennas Propag 2001;49:1683–94.
[6] Liebe HJ, Hufford GA, Cotton MG. Propagation modeling of moist air and suspended water/ice partiles at frequencies below 1000 GHz. In: Proceedings of the AGARD 52nd specialists meeting of the electromagnetic wave propagation panel. Palma de Mallorca, Spain; 1993.
[7] Liebe HJ. MPM—an atmospheric millimeter-wave propagation model. Int J Infrared Millim Waves 1989;10:631–50.
[8] Rosenkranz PW. Water vapor microwave continuum absorption: a comparison of measurements and models. Radio Sci 1998;33:919–28.
[9] Kuhn T, Bauer A, Godon M, Buhler S, Kunzi K. Water vapor continuum: absorption measurements at 350 GHz and model calculations. J Quant Spectrosc Radiat Transfer 2002;74:545–62.
[10] Liebe HJ, Layton DH. Millimeter-wave properties of the atmosphere: laboratory studies and propagation modeling. National Telecommunications and Information Administration , Boulder, Co.; 1987 (NTIA Report 87-224).
[11] Pardo JR, Serabyn E, Cernicharo J. Submillimeter atmospheric transmission measurements on Mauna Kea during extremely dry El Nino conditions: implications for broadband opacity contributions. J Quant Spectrosc Radiat Transfer 2001;68:419–33.

Please cite this article as: Slocum DM, et al. Atmospheric absorption of terahertz radiation and water vapor continuum effects. J Quant Spectrosc Radiat Transfer (2013), http://dx.doi.org/10.1016/j.jqsrt.2013.04.022

[12] Podobedov VB, Plusquellic DF, Fraser GT. Investigation of the water-vapor continuum in the THz region using a multipass cell. J Quant Spectrosc Radiat Transfer 2005;91:287–95.
[13] Podobedov VB, Plusquellic DF, Siegrist KE, Fraser GT, Ma Q, Tipping RH. New measurements of the water vapor continuum in the region from 0.3 to 2.7 THz. J Quant Spectrosc Radiat Transfer 2008;109:458–67.
[14] Podobedov VB, Plusquellic DF, Siegrist KM, Fraser GT, Ma Q, Tipping RH. Continuum and magnetic dipole absorption of the water vapor–oxygen mixtures from 0.3 to 3.6 THz. J Mol Spectrosc 2008;251:203–9.
[15] Burch DE. Absorption of infrared radiant energy by CO_2 and H_2O. III. Absorption by H_2O between 0.5 and 36 cm^{-1} (278 μ–2 cm). J Opt Soc Am 1968;58:1383–94.
[16] Serabyn E, Weisstein EW, Lis DC, Pardo JR. Submillimeter Fourier-transform spectrometer measurements of atmospheric opacity above Mauna Kea. Appl Opt 1998;37:2185–98.
[17] Matsuo H, Sakamoto A, Matsushita S. FTS measurements of submillimeter-wave atmospheric opacity at Pampa la Bola. Publ Astron Soc Japan 1998;50:359–66.
[18] Paine S, Blundell R, Papa DC, Barrett JW, Radford SJE. A Fourier transform spectrometer for measurement of atmospheric transmission at submillimeter wavelengths. Publ Astron Soc Pacific 2000;112:108–18.
[19] Rothman LS, Gordon IE, Barbe A, Chris Benner D, Bernath PF, Birk M, et al. The HITRAN 2008 molecular spectroscopic database. J Quant Spectrosc Radiat Transfer 2009;110:533–72.
[20] Bauer A, Duterage B, Godon M. Temperature dependence of water-vapor absorption in the wing of the 183 GHz line. J Quant Spectrosc Radiat Transfer 1985;36:307–18.
[21] Gordy W, Smith WV, Trambarulo RF. Microwave spectroscopy. Dover Publications; 1953.
[22] Goyette TM, Dickinson JC, Waldman J, Nixon WE. A 1.56 THz compact radar range for W-band imagery of scale-model tactical targets. In: Proceedings of the SPIE Algorithms for Synthetic Aperture Radar Imagery VII, vol. 4053; 2000. p.615–22.
[23] Hoshina H, Seta T, Iwamoto T, Hosako I, Otani C, Kasai Y. Precise measurement of pressure broadening parameters for water vapor with a terahertz time-domain spectrometer. J Quant Spectrosc Radiat Transfer 2008;109:2303–14.
[24] Burch DE, Gryvnak DA, Patty RR. Absorption of infrared radiation by CO_2 and H_2O experimental techniques. J Opt Soc Am 1966;57:885–95.
[25] Greenler RG. Infrared study of adsorbed molecules on metal surfaces by reflection techniques. J Chem Phys 1965;44:310–5.
[26] Van Vleck JH, Weisskopf VF. On the shape of collision-broadened lines. Rev Mod Phys 1945;17:227–36.
[27] Pickett HM, Poynter RL, Cohen EA, Delitsky ML, Pearson JC, Muller HSP. Submillimeter, millimeter, and microwave spectral line catalog. J Quant Spectrosc Radiat Transfer 1998;60:883–90.
[28] Gordy W, Cook RL. Microwave molecular spectra. Wiley-Interscience; 1984.
[29] Bauer A, Godon M. Temperature dependence of water-vapor absoprtion in linewings at 190 GHz. J Quant Spectrosc Radiat Transfer 1990;46:211–20.
[30] Godon M, Carlier J, Bauer A. Laboratory studies of water vapor absorption in the atmospheric window at 213 GHz. J Quant Spectrosc Radiat Transfer 1991;47:275–85.
[31] Bauer A, Godon M, Carlier J, Ma Q, Tipping RH. Absorption by H_2O and H_2O–N_2 mixtures at 153 GHz. J Quant Spectrosc Radiat Transfer 1993;50:463–75.
[32] Bauer A, Godon M, Carlier J, Ma Q. Water vapor absorption in the atmospheric window at 239 GHz. J Quant Spectrosc Radiat Transfer 1994;53:411–23.
[33] Yang Y, Shutler A, Grischkowsky D. Measurement of the transmission of the atmosphere from 0.2 to 2 THz. Opt Express 2011;19:8830–8.

Please cite this article as: Slocum DM, et al. Atmospheric absorption of terahertz radiation and water vapor continuum effects. J Quant Spectrosc Radiat Transfer (2013), http://dx.doi.org/10.1016/j.jqsrt.2013.04.022